

Active acquisition for multimodal neuroimaging

James H Cole[‡], Romy Lorenz[§], Fatemeh Geranmayeh[¶], Tobias Wood[‡], Peter Hellyer[‡], Steven Williams[‡], Federico Turkheimer[‡], Robert Leech[‡]

[‡] Department of Neuroimaging, Institute of Psychiatry, Psychology and Neuroscience, King's College London, London, UK.

[§] MRC Centre for Cognition and Brain Sciences, University of Cambridge, Cambridge, UK; Max Planck Institute for Human Cognitive & Brain Sciences, Leipzig, Germany.

[¶] Faculty of Medicine, Department of Medicine, Imperial College London, London, UK.

Abstract

In many clinical and scientific situations the optimal neuroimaging sequence may not be known prior to scanning and may differ for each individual being scanned, depending on the exact nature and location of abnormalities. Despite this, the standard approach to data acquisition, in such situations, is to specify the sequence of neuroimaging scans prior to data acquisition and to apply the same scans to all individuals. In this paper, we propose and illustrate an alternative approach, in which data would be analysed as it is acquired and used to choose the future scanning sequence: active acquisition. We propose three active acquisition scenarios based around multiple MRI modalities. In Scenario 1, we propose a simple use of near-real time analysis to decide whether to acquire more or higher resolution data or acquire data with a different field-of-view. In Scenario 2, we simulate how multimodal MR data could be actively acquired and combined with a decision tree to classify a known outcome variable (in the simple example here, age). In Scenario 3, we simulate using Bayesian optimisation to actively search across multiple MRI modalities to find those which are most abnormal. These simulations suggest that by actively acquiring data, the scanning sequence can be adapted to each individual. We also consider the many outstanding practical and technical challenges involving normative data acquisition, MR physics, statistical modelling and clinical relevance. Despite these, we argue that by active acquisition allows for potentially far more powerful, sensitive or rapid data acquisition and may open up different perspectives on individual differences, clinical conditions and biomarker discovery.

31 Introduction

32 Neuroimaging involves trade-offs; whether for clinical diagnosis, patient stratification or biomarker
 33 discovery. For example, with a typical MRI scan, there are substantial practical constraints (money,
 34 patient comfort and compliance, radiological reporting) which means decisions have to be taken as to
 35 what kind of scan to perform, where in the brain scan, the scan resolution. The standard approach is to
 36 make these decisions before scanning commences, acquiring the data then analysing it. However, the
 37 optimal resolution/type of scan will depend on what is being investigated and the type and the location
 38 of pathology or abnormalities and may not be known *a priori*.

39 Here, we propose an alternative approach using active learning for real-time optimisation of
 40 neuroimaging data acquisition; providing illustrative examples. Broadly, in our approach data
 41 acquisition and analysis are not separated; instead data is analysed as it is acquired and used to guide
 42 subsequent data acquisition, in a closed-loop. The word game *hangman* is a simple illustration of a
 43 form of active learning (as is predictive text messages and search engine auto-completion): a letter is
 44 guessed, and whether it is present or not is then evaluated; this information is then used to narrow the
 45 search for the next letter. Active learning approaches are potentially far more efficient (in terms of
 46 scanner time) than treating acquisition and analysis as separate phases. A non-active learning version
 47 of hangman would involve guessing all the letters at the start of the game and then evaluating them all
 48 at once without any feedback; in most situations, this would be a highly inefficient strategy.

49 We have previously demonstrated that active learning can be used to guide the choice of experimental
 50 paradigm in functional MRI (Lorenz et al. 2016): with substantial increases in terms of speed,
 51 searching over many experimental parameters far quicker than an exhaustive search. This allows for
 52 far broader research questions to be asked (Lorenz et al. 2018). Active learning also has another
 53 important feature; they involve a prediction and testing cycle, with the learner having to make
 54 predictions that are then tested with out-of-sample data. This potentially increases the replicability of
 55 analyses and reduces the ability for post-hoc bias (Lorenz, Hampshire, and Leech 2017; Lancaster et
 56 al. 2018).

57 The work presented here investigates the use of sequential decision-making to select the type of scan,
 58 using information gained from previous scans actively seek out brain abnormalities or make diagnostic
 59 predictions. This requires data to be collected and analysed in near real-time; however, to illustrate the
 60 potential power of this approach our demonstrations use previously collected data, by simulating the
 61 real-time analysis aspect.

62 Figure 1 presents a video overview of Active Acquisition: (i) scan parameters are chosen (e.g.,
 63 modality or acquisition parameters such as resolution, TR or TE); (ii) the scan is acquired; (iii) pre-
 64 processed; and, (iv) acquired data is compared to an existing normative dataset. The loop then
 65 continues with the information in (iv) used to optimise the next scan (or decide whether sufficient data

have been collected to stop scanning). We explore using Active Acquisition in three different scenarios with T1-weighted MR images:

- 1) Finding a localised structural anomaly (e.g., locating a focal lesion).
- 2) Choosing the optimal scanning modality to actively detect abnormalities.
- 3) Actively choosing the type of scan to characterize an aspect of the individual being scanned (e.g., age).

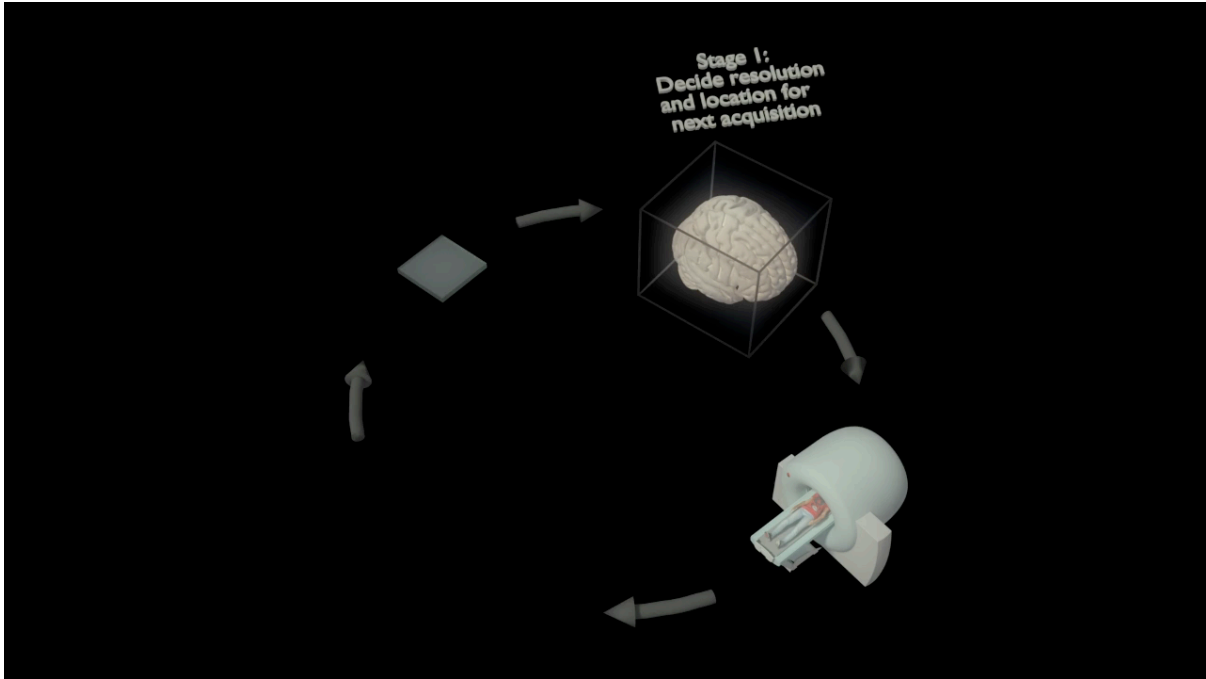


Figure 1: General illustrative video of one active acquisition approach for structural neuroimaging.

75 **Methods**

76 **Scenario 1: Changing structural scan resolution to detect stroke pathology**

77 Our rationale is to start at a low image resolution for a (very rapid) whole brain scan, before acquiring
78 higher resolution scans if the brain appears to be abnormal. This way, it is possible to efficiently image
79 a focal pathology such as a lesion or tumour and to rapidly estimate its spatial location and establish
80 whether more data needs to be acquired, potentially with a restricted field of view focused on the site
81 of the abnormality. Supporting Matlab code can be found in supplementary material.

82 *Choice of scan parameters*

83 For our illustrative simulation, we used existing structural scans (though in practice they would be
84 acquired and analysed online). Practical challenges and limitations to acquiring these data, as well as
85 consider possible methods to mitigate these challenges, as outlined in the Discussion section.

86 At each iteration, the scan is divided into three equally sized volumes, along the z-dimension. The
87 ‘outlier distance’ (defined below) is then quantified for each third by reference to the distribution in
88 an independent normative sample. The volume with the highest outlier distance is then selected and
89 the next scan “acquired”; covering same section of the volume but with the resolution doubled. The
90 process was repeated three times until the maximum resolution of 1mm³ voxel was achieved. The
91 choice of resolution and number of sub-divisions (and other scanner parameters) presented in this
92 scenario is relatively arbitrary. Future work will need to establish the optimal approach for a given
93 clinical or scientific question. There will always be a trade-off between multiple comparisons and
94 precision when assessing; here we chose a very coarse approach which should be sufficient, given the
95 focal and macroscopic nature of the brain injury (i.e., lesion). In clinical or scientific applications, a
96 more sophisticated approach would probably be required, that chooses the brain region for the outlier
97 detection (and potentially subsequent more targeted acquisition), related to the size and location of the
98 pathology or abnormality, possibly changing orientation and the image field-of-view in the process.

99 *Outlier distance from normative sample*

100 The extent to which a participant's image was different from the normative sample was quantified,
101 restricted to the resolution and coverage of the specific scan. The median distance between an
102 individual's scan and each participant in the normative dataset was calculated using the median
103 absolute deviation (in Euclidean distance) of signal intensity averaged across all voxels. This results
104 in a single value of outlier distance. The choice of outlier quantification depends on the type of data
105 being acquired and the question being asked. We opted for the median absolute deviation because it is
106 a simple measure that is relatively robust to violations of normality assumptions. However, we note
107 that many other more sensitive outlier measures could also be used (e.g., measures taking into account
108 covariance across voxels, Fritsch et al. 2012).

109 **Scenario 2: Active multimodal stratification of individual differences**

110 In this scenario, Active Acquisition is used to choose the modality of the scan to achieve a given goal.
111 The rationale is that the optimal scanning modality for assessing an individual, for example to quantify

their relationship to a normative sample, will vary for different individuals; when performing a battery of scans, each individual may have a different set of scans and a different acquisition order.

In Scenario 2, we use multimodal imaging to quantify individual variability. This type of analysis could be relevant when classifying or stratifying individuals into scientifically or clinically relevant groups. To illustrate this, we use the Cam-CAN dataset (Shafto et al. 2014) and with the task of predicting chronological age from neuroimaging data. Predicting age is a useful example case for active multimodal imaging because there are large datasets available, there is little ambiguity about label validity (unlike many clinical descriptions), age is associated with large-scale neural changes (e.g., Good et al. 2001) and “brain-predicted age” has been shown to relate to many other health related biomarkers (e.g., Cole et al. 2018). Cam-CAN is a particularly useful dataset to assess this source of individual variability since the age distribution of the participants is approximately equally balanced across seven decades from 20s to 80s.

To instigate Active Acquisition in this case, we simulate active learning process by fitting a decision tree regression model to the six modalities of Cam-CAN; predictions of chronological age were the outcome measure. This is because: a low-depth decision tree would not include all modalities, just those important for predicting age; makes the decision sequentially (i.e., modality by modality) rather than simultaneously, thus is well-suited for Active Acquisition, and finally; allows different individuals to have different scans and different orders of scans.

A holdout dataset was created with 20% of the individuals, selected randomly (the data partition was performed once rather than pooling across multiple, randomly generated partitions). A decision tree was fit to the remaining 80% of individuals’ six imaging modalities as the predictor variables and their ages in years as the outcome variable. The model hyper-parameters (tree depth, number of leaves, etc.) were estimated with Bayesian optimisation (see supplementary material for Matlab code). Subsequently, the decision tree was evaluated with the holdout participants. The application of the decision tree (the sequential decision process) to each individual in the holdout group, could be performed in real-time to new participants in exactly the same way. For comparison, we also fit a standard support vector regression, with hyper-parameters also optimised with Bayesian optimisation, to the same data (see Matlab code) which used all data modalities simultaneously.

Scenario 3: Active discovery of individual differences with multi-modal imaging

Whereas Scenario 2 focuses on quantifying how an individual varies along some dimension (e.g., age), in Scenario 3, we attempt to actively learn which modality an individual is most likely to be an outlier in. This could be useful for efficiently finding pathology in an individual or for discovering biomarkers; particularly, when there are a large number of possible modalities to choose from and a limited amount of scanning time/participant tolerance of scanning (see supplementary material for code).

To illustrate Scenario 3, we again used the Cam-CAN dataset, as per Scenario 2. In addition, we included a Bayesian optimisation algorithm (Shahriari et al. 2016) to actively learn which modality is most abnormal (as quantified by the magnitude of outlier measurement). Bayesian optimisation is

particularly well suited for this type of problem when the objective underlying function is unknown and costly to evaluate and relatively robust to the presence of noise in the data.

For optimisation to work efficiently, the acquisition function needs to take advantage of existing information; in this case the covariance across individuals for different modalities. Therefore, we split the data into two: 80% of the Cam-CAN participants were used to estimate the space (across modalities) for the algorithm to search across. To do this, we converted each modality to a z-score, then performed a factor analysis (using Matlab) and calculated a single factor. We then reorganized the modalities for the search space for the Bayesian optimisation in terms of weighting on the principle factor; this process estimates how different modalities will co-vary (approximately) with each other. For this example, with only six modalities to choose from, we opted for a simple experiment space with modalities given an integer between 1-6, based on the output of the factor analysis and the optimisation algorithm output integers. For more realistic situations with more complicated spaces (e.g., with many modalities organised along multiple dimensions and with more continuous modalities) one could use alternative (e.g., ratio) scales.

Subsequently, we performed Bayesian optimisation using the remaining 20% of participants, allowing the algorithm to pick the modality for a given individual, with the target objective of finding the minimum z-score. Given the relatively small number of available modalities, we allowed the algorithm to randomly choose three modalities (the burn-in phase) to sample first, to fit a Gaussian process regression and then to use the expected-improvement acquisition function to choose the next point to sample. The expectation was that after some initial random exploration, the model should be able to take advantage of the covariance across individuals to estimate the modality with the minimum z-score more frequently than expected by chance.

To assess whether this optimisation approach was performing above chance levels, we compared results for each individual with the correct factor ordering of modality (based on the covariance structure across individuals) with a random ordering of modalities. For each individual the order of the modalities was randomised (i.e., the ordering of the modalities was no longer based on prior information about how individuals co-vary across modalities). For both random and true covariance models, we calculated the proportion of participants where the optimisation algorithm correctly found the minimum z-score modality. This assessment process was repeated 100 times with different random seeds, allowing different burn-in sampling trajectories for each individual for each iteration.

Data acquisition

In Scenario 1, data were acquired from 13 participants: seven healthy controls with no history of neurological problems (average age= 56, range = 46 to 67, female=4); and, six patients with chronic left-hemisphere middle-cerebral artery focal strokes (average age= 60, range = 47 to 78, female=2, average lesion volume= 10.6 cm³). For each participant, three T1-weighted scans were acquired at different voxel resolutions: 1mm³, 2mm³, 4mm³. As with other data presented here, the patient and control data were not collected in real-time but is intended to illustrate the general utility of the approach. In this example, we use seven healthy controls as a “normative” sample; this is, obviously,

far too small for actual practical uses, but was limited by the data set available (multiple resolutions per individual) but does illustrate the potential of the approach if scaled-up.

For Scenarios 2 and 3, multimodal MRI data from 611 people (age range from 18-88, 312, female) were taken from the Cam-CAN dataset. This data consisted of T1-weighted, T2-weighted, diffusion-weighted MRI, three functional scans (resting-state fMRI, movie-watching fMRI and a blocked sensorimotor task-based fMRI). Imaging acquisition has been presented in detail elsewhere (Shafto et al. 2014).

Image pre-processing

Scenario 1:

To explore the feasibility of processing brain images in near real-time and to make minimal assumptions about the location or nature of pathology when calculating outlier distance, we used very simple and rapid pre-processing. T1-weighted images were converted from DICOM to NifTI format before being linearly-registered into MNI152 1mm³ space using the very efficient registration tool NiftyReg (Modat 2012). The same process was performed for each of the three different image resolutions acquired.

Scenario 2 & 3:

T1-weighted MRI

All T1-weighted structural images from all three datasets were processed in the same way as follows. Grey matter (GM), white matter (WM) and cerebrospinal fluid (CSF) volumes were calculated using SPM12 ‘Segment’ (University College London, UK). Voxelwise assessment of changes to brain volume was calculated using the SPM symmetric diffeomorphic registration process (Ashburner 2007) to a predefined template used in our previous studies (Cole et al. 2018).

For the Cam-CAN dataset, the other modalities were (briefly) processed as detailed below. These analyses are merely illustrative of the type of data that could be extracted; they have been simplified from multivariate raw data for each individual into a single summary statistic, chosen for its simplicity rather than because it is optimal for measuring individual variability.

Diffusion-weighted MRI

White-matter microstructure was analysed under the diffusion tensor imaging (DTI) paradigm, using FSL (<http://fsl.fmrib.ox.ac.uk/>) tract-based spatial statistics (Smith et al. 2006) with DTI-TK (Zhang et al. 2007) software for affine then non-linear tensor-based image registration. Normalised tensor images were used to derive voxelwise measures of fractional anisotropy (FA) and mean diffusivity.

219 Mean values across major WM fibre tracts, taken from the JHU-ICBM tract atlas, were calculated,
220 resulting in an FA average value per individual.

221 *T2-weighted MRI*

222 The same diffeomorphic transformation that was calculated for the grey matter was applied to the T2-
223 weighted scan data to warp each individual's data into the same T1-weighted template space.
224 Subsequently, the average T2-weighted intensity values from the normalised image was calculated.

225 *Resting state functional connectivity*

226 Measures of 'within-network' connectivity were calculated from resting-state fMRI data using FSL
227 'Dual Regression' (Filippini et al. 2009). Prior to the dual regression, standard FSL 'MELODIC'
228 analysis pipeline was applied (Smith et al. 2004): high-pass temporal filtering at 100s, spatial
229 smoothing at 5mm FWHM, global intensity normalisation, motion-correction followed by realigning
230 the data into MNI152 space using linear registration before the data were resampled into 4x4x4mm
231 voxel space. Then the data were cleaned by linearly regressing six motion parameters from each
232 voxel's time-course, before nuisance WM and CSF time-courses were linearly regressed from each
233 voxel (using average CSF and WM masks from the segmentation). Subsequently, using canonical
234 spatial maps of twenty networks (including both intrinsic connectivity networks and likely noise
235 networks) (Smith et al. 2009), cleaned data underwent a multiple regression to derive voxelwise
236 measures of connectivity for each network for each individual. Finally, to keep this aspect of the
237 approach as simple as possible, we averaged all voxels within the default mode network (DMN) mask;
238 this process resulted in an individualized 'within-network' connectivity measure for the DMN. Future
239 work (with any fMRI data) could explore only using short segments of the functional time-series
240 (rather than the whole scan), to allow for faster, repeated measurements.

241 *Movie-watching functional connectivity*

242 This was identical to the analysis of the resting state connectivity, calculating individualised within-
243 DMN functional connectivity while watching the movie.

244 *Task fMRI*

245 The sensorimotor task data were analysed following a standard FSL pipeline: global intensity
246 normalisation, high-pass temporal filtering at 100s, spatial smoothing at 5mm FWHM, motion-
247 correction, registration of the data into MNI152 space using linear registration. Subsequently, a general
248 linear model was applied voxelwise (using the standard FSL approach for dealing with the auto-
249 correlation of residuals (Smith et al. 2004)), with separate explanatory variables modelling auditory
250 and visual blocks convolved with a canonical hemodynamic response function. Subsequently, a
251 contrast of all task conditions versus the implicit baseline was calculated and a higher-level group
252 mixed-effects model was used to calculate increased and decreased BOLD activity with task. This
253 resulted in group task positive and task negative networks which were converted into binary mask
254 defined by voxels that survived cluster correction for multiple comparisons. An individualised task

fMRI measure was calculated by taking the average activity within the positive network mask and subtracting the average value from the negative network mask.

Results

Scenario 1: Changing structural scan resolution to detect stroke pathology

The simplest Active Acquisition model involves starting with a rapid, low resolution structural scan, analysing it and then deciding to whether to acquire further higher-resolution scan(s). Here, we collected lower-resolution (4mm^3) structural scans from six patients with focal brain lesions and seven age-matched controls, followed by intermediate-resolution (2mm^3) and higher-resolution (1mm^3) scans. An illustrative patient at three resolutions is presented in Figure 1 (left). Even with the lowest resolution scan, patients and control participants (Figure 1 - right) show a large difference in terms of outlier distance. This example, in patients with large focal strokes, illustrates how data simple measures calculated in near real time, and then a decision made as to whether a slower, higher resolution scan is needed or not. As can be seen from the outlier measurements, only a subset of the control participants, close to the boundary with the patients would require slower, additional scans.

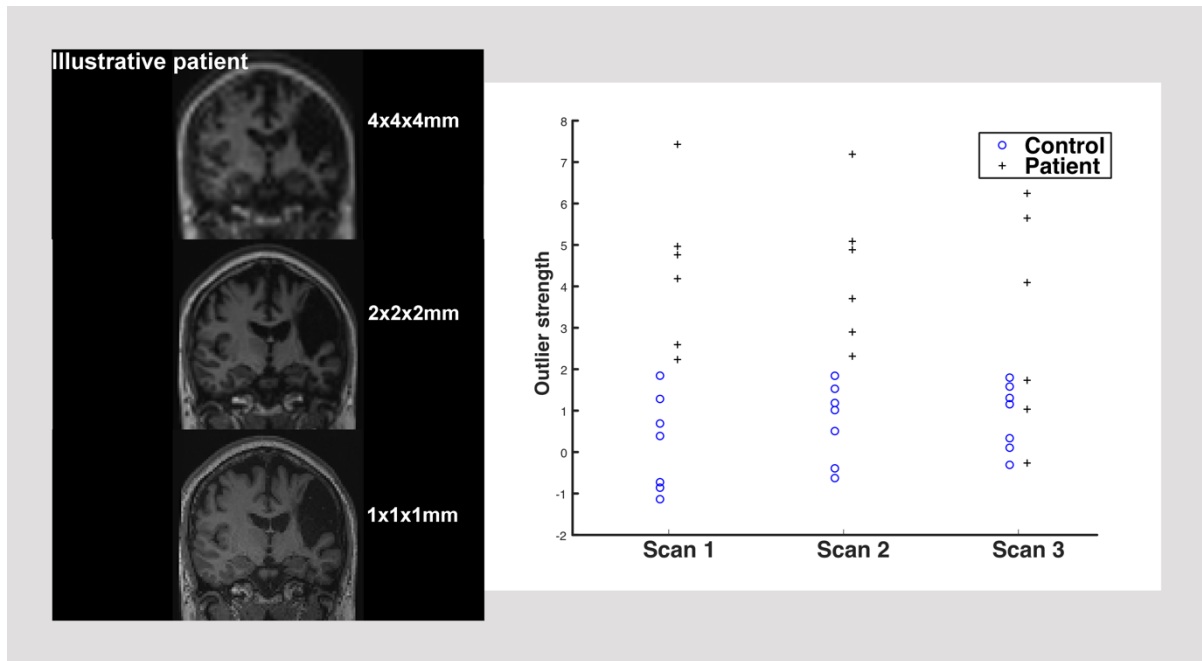


Figure 2: Left, a stroke patient with three different resolution T1-weighted scans. Right, outlier distance from control participants, for each participant for the three different scans, and combining all three scans. For each scan, the scan is subdivided into three, and the maximum outlier distance (out of the three subdivisions assessed) from the control data is plotted. This shows a relatively clear difference in outlier distance between patients and controls. For most patients and controls (either far from 0 or close to 0 respectively), there is no need to collect additional higher resolution (slower) scans to differentiate the two groups.

We also simulated optimising the scan field-of-view in near-real-time. In this case, at each resolution the brain is divided into thirds and the negative outlier distance calculated for each third. The third that is most strongly classed as an outlier is then retained and subsequent, higher resolution scans, acquired just within that third. The process then repeats (Figure 3, top). This illustrates how a composite brain

image can be built up out of increasing resolution scans. This could trade-off sensitivity for tissue contrast with increasing quantification of brain structure, while limiting scanning time.

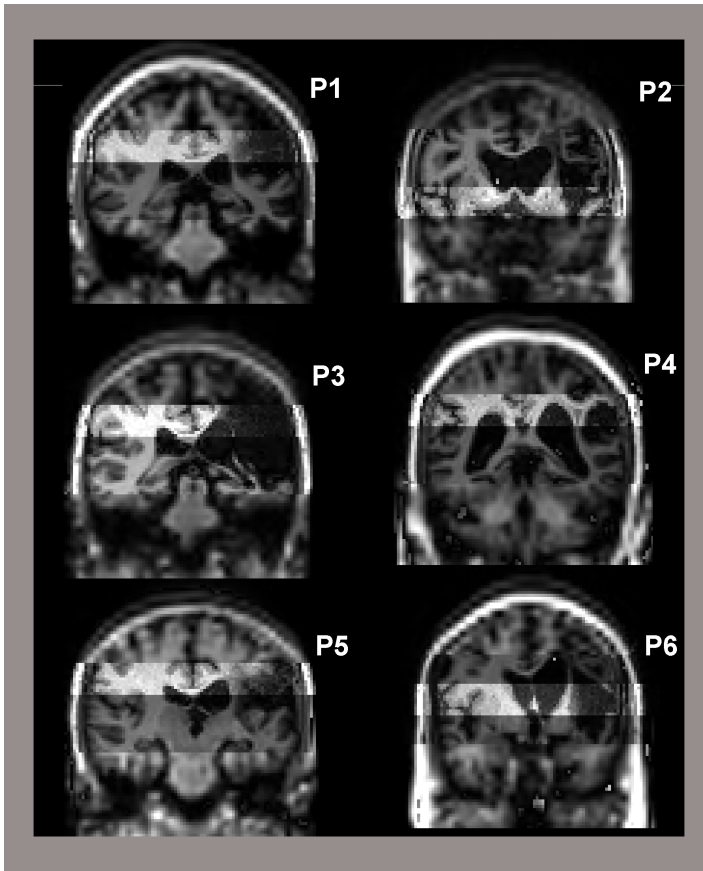


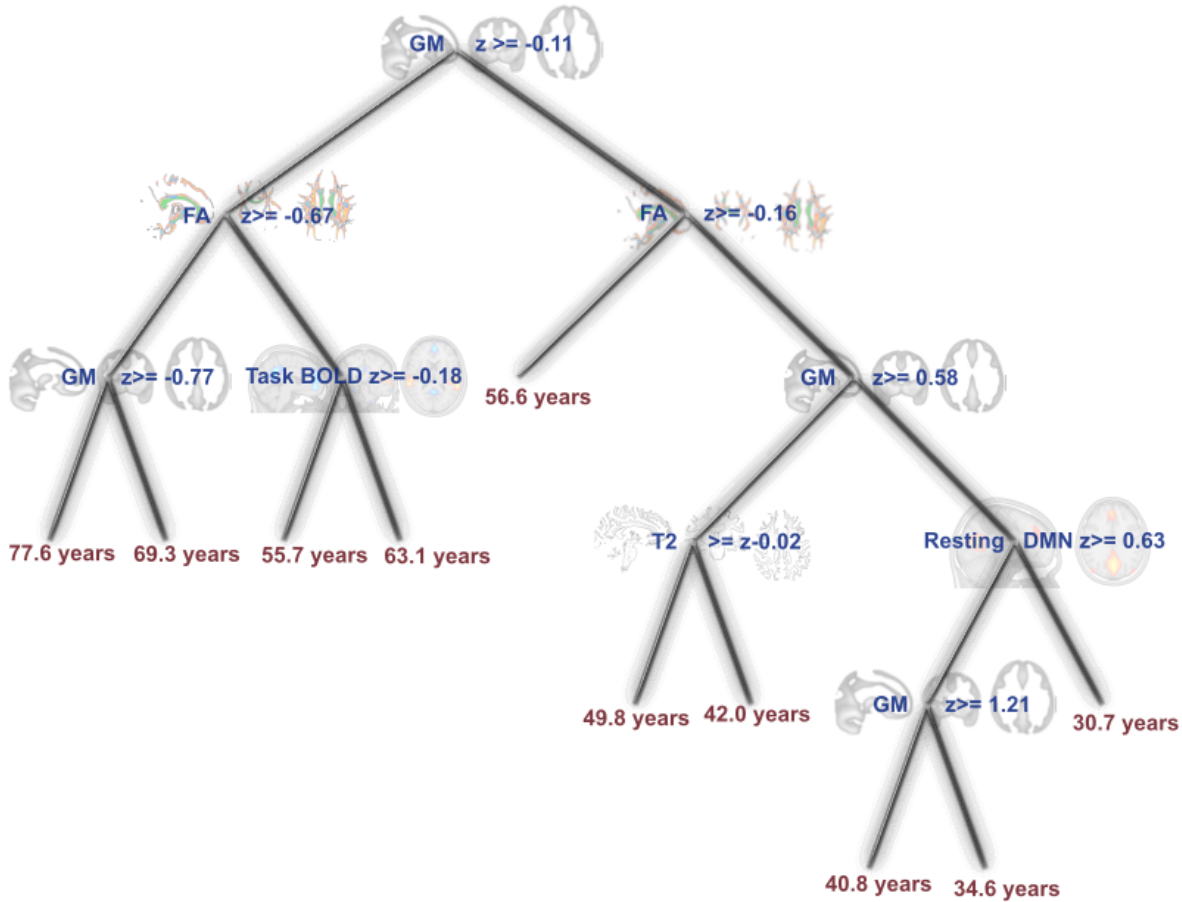
Figure 3: top, composite coronal slices (one for each of the six patients), built out of increasing resolution with different coverage T1-weighted scans, restricting the scan volume to that quantified as most abnormal relative to the controls. This demonstrates that the very simple approach to subdividing the brain and quantifying outliers can be used to ‘zoom’ in on areas of pathology that are specific for individual patients.

Scenario 2: Active multimodal stratification of individual differences

When fitting the decision tree regression to predict chronological age from neuroimaging data, the regression model contained multiple modalities (indicating its utility in a sequential acquisition and analysis procedure). It started with GM volume, consistent with previous data suggesting a strong relationship between GM and age (Good et al. 2001), with lower z-scores indicating older age. Subsequently, average WM FA was chosen, again with lower values relating to older age. Next, the model’s branches become very different, both in terms of modality chosen and number of scans required, depending on the route through the tree.

We observed that the mean absolute error (MAE) of age prediction is 10.47 years and the median error 8 years. For comparison, the MAE calculated on the same data using a support vector regression approach with all of the data is very similar, was 10.42 years, with a median error of 9.4 years. The predicted age performance is considerably worse than has been reported elsewhere for single modalities from the same dataset e.g., (Lancaster et al. 2018); this is to be expected given that, for illustrative simplicity, we have collapsed large, multivariable datasets into single summary statistics (i.e., a single value for grey matter probability per individualm etcetera). In practice, sequential

302 decision methods incorporating multivariate datasets to utilise the full richness of the underlying data
 303 are needed to realise the potential of the approach.



304
 305 Figure 4: The decision tree regression model calculated on summary statistics for each of six modalities to
 306 predict individual age. At each node in the tree the z-scored data for a given individual are used to decide
 307 modality to use next or whether to stop at this point. This can happen in near-real time, with different individuals
 308 taking different routes through the tree, and with different numbers of scans. The estimated age is then
 309 approximated by the age at the leaf nodes.

310 Scenario 3: Active discovery of individual differences with multi-modal imaging

311 Here we simulated closed-loop Bayesian optimisation used to discover the modality for a given
 312 individual (from the holdout dataset) where the negative outlier distance is most (i.e., relative to
 313 normative data from the training dataset), shown in Figure 5. For the optimisation to work efficiently
 314 (i.e., faster than exhaustive search across modalities), it needs to take advantage of covariance across
 315 modalities in individual differences. In Figure 5A, the order of modalities (Movie, Rest, Task, T2, FA,
 316 GM) reflects this covariance structure. This provides prior information that the optimisation algorithm

can combine with some random initial samples (numbers 1-3 in Figure 5A, left) to build a Gaussian process regression model to predict the modality with minimum z-score (in this case number 4, T2). By chance, the proportion of participants for whom the algorithm finds the modality with the minimum z-score is 0.67 (given that it sampled four modalities in total). When the Bayesian optimisation algorithm utilises the estimated covariance structure from the training dataset, the proportion increases to >0.72 on average (results in Figure 5B are presented from 100 replications). We see that if the modality ordering is chosen randomly (rather than based on covariance across individuals from the training set) the average proportion of participants where the minimum modality is selected approximates that expected by chance (i.e., 0.67). We also see that this translates into an increase in the estimated minimum z-score found when using the optimisation algorithm compared to the random modality ordering. This difference between true and random ordering of modality search space is relatively modest (approximately 5%). However, the dataset used in this example has very few modalities and thus a restricted search space and has a relatively limited sample size. Also, we used somewhat coarse pre-processing and summary statistics. Applying this approach to on-going data collection in much larger projects or at clinical neuroimaging centres that scan large numbers of people, alongside the myriad of different MRI scan modalities available, means that this approach could be substantially improved and used much more powerfully for biomarker discovery.

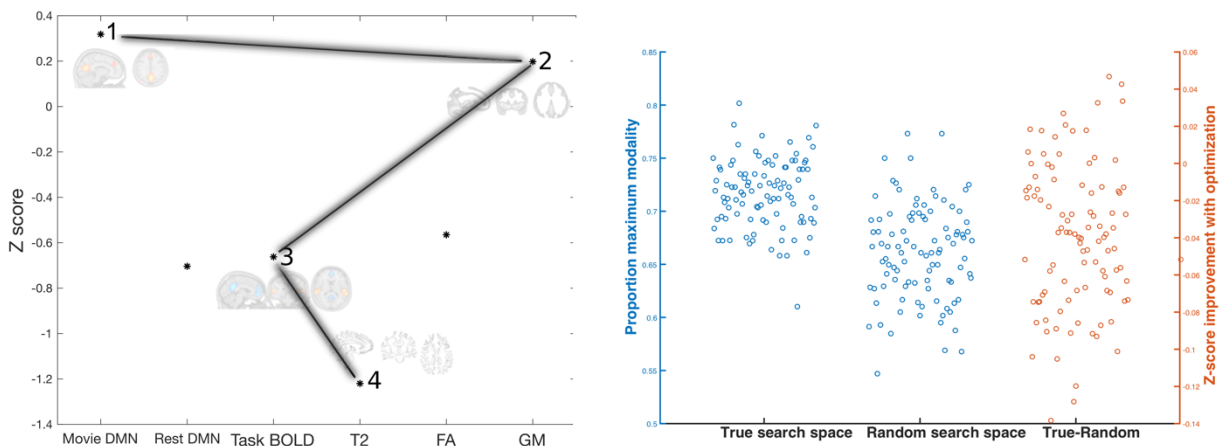


Figure 5: Active discovery of individual differences across modalities, controlled by a closed-loop optimisation algorithm. Left, the trajectory of the algorithm as it traverses the modality space, estimating a model of which modalities a specific individual appears most abnormal in, without exhaustively sampling every point, before guessing which is the most abnormal. Right, proportion of participants in the holdout set where the optimisation algorithm correctly chose the modality most sensitive to abnormalities for both true and random modalities, and

the decrease in estimated minimum z-statistic for true versus random organisation of modalities (repeated 100 times with different burn-in random initialisation of the models).

Discussion

Here we outlined the Active Acquisition approach for optimising multimodal neuroimaging scan protocols. The examples are intended to illustrate the potential utility of Active Acquisition; by using this approach important decisions about the scan do not need to be in advance; how long to scan for, what modalities to acquire, which regions of the brain to focus on. Rather, the precise nature of the scanning protocol is determined online, adapting to the individual in the scanner, optimising acquisition for a given set of circumstances. Our current goal has been to outline several broad scenarios that suggest how Active Acquisition could progress and its general potential, rather than provide evidence of a specific biomarker or indeed specific pipelines or analysis approaches. Here, we discuss future potential directions for Active Acquisition, in particular for diagnosis and stratification as well as for biomarker discovery. We envisage these two directions developing along independent but complementary lines. We also consider some practical issues that need to be overcome to take the approach forward and maximise its potential for clinical and scientific neuroimaging.

Clinical diagnosis

Perhaps the more obvious use case for Active Acquisition is in clinical diagnostics and the stratification of individuals into subgroups. Incorporating Active Acquisition could lead to either shorter scanning sessions, or more accurate and more reliable data collection. Multiple imaging modalities are typically collected in a diagnostic clinical scanning session, many of which end up being unnecessary for accurate diagnosis. If the scanning session can be terminated early, when sufficient diagnostic certainty has been reached (as in Scenario 1), there would be a significant reduction in scanning time, reducing patient discomfort and scanning costs. Equally, by optimising the order of the scans (as in Scenario 2), tailored to the targeted disorder, this would potentially remove the need to collect all modalities, leading to the same benefits in terms of time, cost and patient comfort.

Alternatively, Active Acquisition could be used to produce more accurate diagnoses and to optimise certain modalities for clinical use that are currently not used in clinical settings. Active Acquisition could make use of scanning time and resources more efficient; collecting repetitions of important scans (until a sufficient signal-to-noise ratio has been reached) or changing the scanning resolution or field-of-view to focus on potential abnormalities. This may be of particular use in relatively low signal-to-noise imaging modalities. For example, the pattern of brain damage presented Scenario 1 (focal ischaemic stroke) is evident even on very low resolution and low signal-to-noise structural scans; however, other neurological conditions may have far more subtle abnormalities and other modalities (e.g., arterial spin labelling, diffusion tensor imaging, resting state or task BOLD scans) have lower signal-to-noise, and may benefit from more spatially focused, repeated data acquisition.

A pertinent issue facing neuroimaging research in clinical samples is how to deal with heterogeneity within patient groups; particularly common in chronic neuropsychiatric diseases. The “average” best scanning protocol sequence may well not be optimal at identifying clinically relevant abnormalities in a specific individual. Potentially, different scans may be optimal for a given diagnosis in different individuals and at different points in the natural history of a disease. One major strength of Active

380 Acquisition approaches is that they can more easily locate an individual patient’s “sweet-spot” from a
 381 large menu of possible scan types/parameters in a time-efficient manner, without having to
 382 exhaustively search through all possibilities.

383 *Biomarker discovery*

384 Finding biomarkers that sensitively detect individual variability linked to clinical and scientific
 385 questions is an important precursor to improving diagnosis and stratification. The application of Active
 386 Acquisition illustrated in Scenario 3 presents a radically different way to achieve this: actively
 387 searching for modalities or scanning parameters give abnormal readouts for a single individual. This
 388 approach contrasts with the current typical approach to biomarker discovery which can be
 389 characterised as choosing a set of modalities prior to scanning that are thought to be related to the
 390 clinical question and then assessing them on a large group of patients and controls or subgroups of
 391 patients, to provide sufficient statistical power to detect average group differences. Active Acquisition
 392 also has the benefit of attempting to focus on modalities only when they are likely to be abnormal for
 393 an individual relative to a normative dataset, which is potentially much more powerful than the
 394 comparison of group averages, as well as leading intuitively to clinical applications of personalised
 395 medicine. Active Acquisition also has the advantage of relying less on relatively arbitrary decisions
 396 that lead to a limited number of modalities being acquired, which means that the clinically-relevant
 397 sweet-spot for data acquisition is more likely to be found.

398 Active acquisition could also avoid the potential problem of scanning protocols being determined
 399 based on biased or inaccurate previous studies. Given the replication ‘crisis’ in biomedical research,
 400 such issues are becoming increasingly recognised as a serious problem in medical imaging. Active
 401 optimisation approaches (such as in Scenario 3) involve repeatedly cycling between prediction and
 402 hypothesis testing on out-of-sample data, and as such are less susceptible to data overfitting. Equally,
 403 active optimisation approaches like these also involve a form of implicit “pre-registration” (Lorenz,
 404 Hampshire, and Leech 2017). This makes it harder to engage in certain questionable research practices
 405 (e.g., p-hacking, post-hoc hypothesising (Poldrack et al. 2017)) that are currently thought to hamper
 406 the development of neuroimaging biomarkers.

407 One additional advantage of active optimisation is that it is able to estimate how an individual varies
 408 from normality across the whole of the search space, despite only sampling a subset of the modalities
 409 tested included in the space. While the gains observed were relatively minor in the current example,
 410 where only six modalities organised along one searchable dimension were considered, the potential
 411 benefit would grow as the space becomes larger and multidimensional. Using the optimisation
 412 algorithm to map out the entire possible space offers the potential for a very rich, but efficiently
 413 collected, description of how an individual differs from normality. The search space mapped out could
 414 involve observing multiple optima in a given individual and estimating modalities with higher and
 415 lower than typical signal. Subsequent offline higher-level modelling (e.g., clustering or other data
 416 reduction approaches) could then be applied across individuals to find frequent patterns of abnormality
 417 from across all modalities.

418 *Need for different types of normative datasets*

419 One major limiting step to the development of Active Acquisition is the need to have well-
 420 characterised variability across individuals in both healthy or ‘normal’ participants as well as clinical

samples and relevant subgroups. Achieving this will require developing large datasets from which to derive estimates of between-individual covariance.

Some simpler applications of Active Acquisition could be built with existing normative datasets. For example, when the problem involves deciding when to stop collecting more data because a sufficient signal-to-noise ratio has been reached, increasing confidence in the inferences made from these data. Other approaches could take advantages of new acquisition methods such as the very rapid multi-contrast images at the start of a scan (Skare et al. 2018) or synthetic imaging which are then used to decide whether to collect slower, higher resolution scans. To utilise these types of scans, existing datasets could be utilised to create sufficiently large normative models.

However, for other applications, such as when searching across modalities (Scenarios 2 and 3), the benefits of Active Acquisition may be most evident when the space of possible modalities/parameters to be considered is large but structured in some way. Indeed, while at present only a small number of imaging modalities are employed clinically, more modalities could be useful but only for stratifying specific subgroups. An accurate understanding of the covariance between modalities/scan parameters relevant to the clinical or scientific question will be necessary for maximising the benefit from these approaches

In Scenario 3, where the optimisation algorithm maps out where an individual is maximally abnormal, understanding the covariance across imaging modalities in a healthy control group (possibly controlling for factors such as age) may suffice. Existing large-scale projects to produce large normative databases have focused on small numbers of modalities collected in large numbers of people (e.g., UK Biobank (Sudlow et al. 2015), Human Connectome Project (Van Essen et al. 2013) and the Cam-CAN dataset presented here). One possible approach is to use meta-analyses of different imaging modalities to try to estimate covariance structure across modalities (capitalising on the fact that different large-scale projects have some shared modalities but also differ from each other). An even better approach would be to have large-scale data collection projects that explicitly seek to quantify covariance across many different imaging modalities/scan parameters. Ideally, this would involve many different representative individuals being scanned, but each with different subsets of modalities/scan parameters; subsequently, a large, comprehensive covariance matrix across individuals can be assembled out of the incomplete datasets from each individual. These normative datasets will allow active searching for how individual patients vary from normality across many modalities, useful for biomarker discovery, without requiring dedicated large multimodal datasets for each clinical condition. Approaches such as Bayesian optimisation with Gaussian processes will allow us to start with relatively few assumptions (i.e., only approximate similarity across modalities near each other in the experimental search space which can be based on health control data); importantly, the approach should work for individuals even when there are areas of the experimental space that deviate from the normative data.

There are also likely to be some situations, however, where acquiring targeted multi-modal normative datasets for specific clinical conditions will also be important. For example, when performing diagnostics rather than discovery of biomarkers (more like in Scenario 2). In these situations, bespoke multimodal datasets may be necessary to arrive at a very specific quantification of the covariance between different modalities, in order to accurately guide the sequential decision making. In such

situations, particularly, with rare disease groups, acquisition of such datasets would be far more challenging and may not be practical.

Methodological considerations

All methodological approaches come with costs and benefits; with active acquisition approaches one concern is that early mismeasurement can lead to serious failures later on. For example, in Scenario 1, this could result in terminating scans prematurely without collecting sufficient data; or, e.g., in Scenario 2, this could involve travelling down the wrong branch of the decision tree. In such situations, important information for diagnosis or biomarker discovery may not be collected. This cost of using active approaches will be most acute when the underlying covariation between scan modalities is well understood and the optimal scan type is known. In contrast, the way that we currently collect data in many exploratory studies (e.g., UK Biobank), it is likely that optimal scans for assessing variability in an individual are being omitted. This reflects the classic exploration versus exploitation trade off well-known in computer science.

For the benefits of active exploration to be maximised, many choices have to be made regarding the acquisition function to guide exploration, how to decide when to stop searching, how to quantify abnormality or predict an individual's classification. We have suggested several simple illustrative scenarios, but each comes with its own specific challenges and future directions. There is long history of methodological developments for adaptive studies in clinical situations (Cornfield, Halperin, and Greenhouse 1969) (Hauskrecht and Fraser 2000)(Alagoz et al. 2010). Future work is needed to incorporate some of the more sophisticated approaches developed in these other domains to neuroimaging and ideally combine them multivariate classification and clustering approaches increasingly commonly used with MRI. In Scenarios 2 and 3, work is needed to understand what happens when there is not a single optimum modality to maximally quantify abnormality (Scenario 3) or multiple equally good paths through the decision tree (Scenario 2). Future work is also needed to evaluate how to robustly quantify the abnormality of an individual's scan, considering the large number of voxels and possibly heterogeneous or diffuse pathologies. Equally, future work is needed to develop rapid and robust image pre-processing, so that it can occur in near real-time. Recent developments in deep learning offer promise, where for example a structural MR image can undergo an analogue of a complete pre-processing pipeline in a matter of seconds (Cole et al. 2017).

Finally, from an MR physics perspective, there are also a number of limitations and challenges. Actively altering the field-of-view and resolution (as suggested in Scenario 1 where the scan zooms in on the site of injury) for 3D structural imaging may not have any benefits (in terms of time saved, increased resolution) given inherent trade-offs between tissue contrast, signal to noise and number of measurements acquired. However, a similar approach could be taken with other imaging modalities (e.g., arterial spin labelling, diffusion imaging) where increased signal to noise from restricting the number of slices or increasing the resolution may be beneficial. Equally, there may be different sources of information that different resolutions and fields-of-view could acquire (e.g., rapidly assessing geometry at higher resolution and tissue contrasts at a lower resolution).

In summary, here we have presented active acquisition, a novel conceptual approach to how neuroimaging data could be collected. We have utilised advances in optimisation algorithms and harnessed large publicly-available neuroimaging databases to develop active acquisition. This

approach embeds data analysis into the acquisition process, allowing information to be obtained and employed for making online decisions about the optimal scans or parameters for a given clinical or scientific goal. While active acquisition is still at the embryonic stage, our intention with this manuscript and the illustrative examples contained herein, is to provide the groundwork for future conceptual and experimental work aimed at optimising the acquisition of neuroimaging data for clinical and scientific purposes.

Acknowledgements

Matlab code for the illustrative scenarios presented in this work can be found at <https://github.com/ActiveNeuroImaging/MultimodalActiveAcquisition>. The best way to view the paper is to download the PDF from the github repository .

James Cole is funded by a UKRI Innovation Fellowship and a Wellcome Trust Seed Award in Science. Robert Leech is supported by MRC Research grant MR/R005370/1.

References

- Alagoz, Oguzhan, Heather Hsu, Andrew J. Schaefer, and Mark S. Roberts. 2010. "Markov Decision Processes: A Tool for Sequential Decision Making under Uncertainty." *Medical Decision Making* 30 (4): 474–83.
- Ashburner, John. 2007. "A Fast Diffeomorphic Image Registration Algorithm." *Neuroimage* 38 (1): 95–113.
- Cole, J. H., S. J. Ritchie, M. E. Bastin, M. C. Valdés Hernández, S. Muñoz Maniega, N. Royle, J. Corley, et al. 2018. "Brain Age Predicts Mortality." *Molecular Psychiatry* 23 (5): 1385–92. <https://doi.org/10.1038/mp.2017.62>.
- Cole, James H., Matthan WA Caan, Jonathan Underwood, Davide De Francesco, Rosan A. van Zoest, Ferdinand WNM Wit, Henk JMM Mutsaerts, Rob Leech, Gert J. Geurtsen, and Peter Portegies. 2018. "No Evidence for Accelerated Ageing-Related Brain Pathology in Treated HIV: Longitudinal Neuroimaging Results from the Comorbidity in Relation to AIDS (COBRA) Project." *Clinical Infectious Diseases*.
- Cornfield, Jerome, Max Halperin, and Samuel W. Greenhouse. 1969. "An Adaptive Procedure for Sequential Clinical Trials." *Journal of the American Statistical Association* 64 (327): 759–70.
- Filippini, Nicola, Bradley J. MacIntosh, Morgan G. Hough, Guy M. Goodwin, Giovanni B. Frisoni, Stephen M. Smith, Paul M. Matthews, Christian F. Beckmann, and Clare E. Mackay. 2009. "Distinct Patterns of Brain Activity in Young Carriers of the APOE-E4 Allele." *Proceedings of the National Academy of Sciences* 106 (17): 7209–14.
- Fritsch, Virgile, Gaël Varoquaux, Benjamin Thyreau, Jean-Baptiste Poline, and Bertrand Thirion. 2012. "Detecting Outliers in High-Dimensional Neuroimaging Datasets with Robust Covariance Estimators." *Medical Image Analysis*, Special Issue on the 2011 Conference on

- 539 Medical Image Computing and Computer Assisted Intervention, 16 (7): 1359–70.
540 <https://doi.org/10.1016/j.media.2012.05.002>.
- 541 Good, C. D., I. S. Johnsrude, J. Ashburner, R. N. Henson, K. J. Friston, and R. S. Frackowiak. 2001.
542 “A Voxel-Based Morphometric Study of Ageing in 465 Normal Adult Human Brains.”
543 *NeuroImage* 14 (1 Pt 1): 21–36. <https://doi.org/10.1006/nimg.2001.0786>.
- 544 Hauskrecht, Milos, and Hamish Fraser. 2000. “Planning Treatment of Ischemic Heart Disease with
545 Partially Observable Markov Decision Processes.” *Artificial Intelligence in Medicine* 18 (3):
546 221–44.
- 547 Lancaster, Jenessa, Romy Lorenz, Rob Leech, and James H. Cole. 2018. “Bayesian Optimization for
548 Neuroimaging Pre-Processing in Brain Age Classification and Prediction.” *Frontiers in Aging
549 Neuroscience* 10: 28. <https://doi.org/10.3389/fnagi.2018.00028>.
- 550 Lorenz, Romy, Adam Hampshire, and Robert Leech. 2017. “Neuroadaptive Bayesian Optimization
551 and Hypothesis Testing.” *Trends in Cognitive Sciences* 21 (3): 155–67.
552 <https://doi.org/10.1016/j.tics.2017.01.006>.
- 553 Lorenz, Romy, Ricardo Pio Monti, Inês R. Violante, Christoforos Anagnostopoulos, Aldo A. Faisal,
554 Giovanni Montana, and Robert Leech. 2016. “The Automatic Neuroscientist: A Framework
555 for Optimizing Experimental Design with Closed-Loop Real-Time FMRI.” *NeuroImage* 129
556 (April): 320–34. <https://doi.org/10.1016/j.neuroimage.2016.01.032>.
- 557 Lorenz, Romy, Ines R. Violante, Ricardo Pio Monti, Giovanni Montana, Adam Hampshire, and Robert
558 Leech. 2018. “Dissociating Frontoparietal Brain Networks with Neuroadaptive Bayesian
559 Optimization.” *Nature Communications* 9 (1): 1227. [https://doi.org/10.1038/s41467-018-](https://doi.org/10.1038/s41467-018-03657-3)
560 03657-3.
- 561 Modat, Marc. 2012. “Efficient Dense Non-Rigid Registration Using the Free-Form Deformation
562 Framework.” UCL (University College London).
- 563 Poldrack, Russell A., Chris I. Baker, Joke Durnez, Krzysztof J. Gorgolewski, Paul M. Matthews,
564 Marcus R. Munafò, Thomas E. Nichols, Jean-Baptiste Poline, Edward Vul, and Tal Yarkoni.
565 2017. “Scanning the Horizon: Towards Transparent and Reproducible Neuroimaging
566 Research.” *Nature Reviews Neuroscience* 18 (2): 115.
- 567 Shafto, Meredith A, Lorraine K Tyler, Marie Dixon, Jason R Taylor, James B Rowe, Rhodri Cusack,
568 Andrew J Calder, et al. 2014. “The Cambridge Centre for Ageing and Neuroscience (Cam-
569 CAN) Study Protocol: A Cross-Sectional, Lifespan, Multidisciplinary Examination of Healthy

- 570 Cognitive Ageing.” *BMC Neurology* 14 (October). [https://doi.org/10.1186/s12883-014-0204-](https://doi.org/10.1186/s12883-014-0204-1)
571 1.
- 572 Shahriari, Bobak, Kevin Swersky, Ziyu Wang, Ryan P. Adams, and Nando De Freitas. 2016. “Taking
573 the Human out of the Loop: A Review of Bayesian Optimization.” *Proceedings of the IEEE*
574 104 (1): 148–75.
- 575 Skare, Stefan, Tim Sprenger, Ola Norbeck, Henric Rydén, Lars Blomberg, Enrico Avventi, and
576 Mathias Engström. 2018. “A 1-minute Full Brain MR Exam Using a Multicontrast EPI
577 Sequence.” *Magnetic Resonance in Medicine* 79 (6): 3045–54.
- 578 Smith, Stephen M., Peter T. Fox, Karla L. Miller, David C. Glahn, P. Mickle Fox, Clare E. Mackay,
579 Nicola Filippini, Kate E. Watkins, Roberto Toro, and Angela R. Laird. 2009. “Correspondence
580 of the Brain’s Functional Architecture during Activation and Rest.” *Proceedings of the*
581 *National Academy of Sciences* 106 (31): 13040–45.
- 582 Smith, Stephen M., Mark Jenkinson, Heidi Johansen-Berg, Daniel Rueckert, Thomas E. Nichols, Clare
583 E. Mackay, Kate E. Watkins, Olga Ciccarelli, M. Zaheer Cader, and Paul M. Matthews. 2006.
584 “Tract-Based Spatial Statistics: Voxelwise Analysis of Multi-Subject Diffusion Data.”
585 *Neuroimage* 31 (4): 1487–1505.
- 586 Smith, Stephen M., Mark Jenkinson, Mark W. Woolrich, Christian F. Beckmann, Timothy EJ Behrens,
587 Heidi Johansen-Berg, Peter R. Bannister, Marilena De Luca, Ivana Drobnyak, and David E.
588 Flitney. 2004. “Advances in Functional and Structural MR Image Analysis and Implementation
589 as FSL.” *Neuroimage* 23: S208–19.
- 590 Sudlow, Cathie, John Gallacher, Naomi Allen, Valerie Beral, Paul Burton, John Danesh, Paul Downey,
591 Paul Elliott, Jane Green, and Martin Landray. 2015. “UK Biobank: An Open Access Resource
592 for Identifying the Causes of a Wide Range of Complex Diseases of Middle and Old Age.”
593 *PLoS Medicine* 12 (3): e1001779.
- 594 Van Essen, David C., Stephen M. Smith, Deanna M. Barch, Timothy EJ Behrens, Essa Yacoub, Kamil
595 Ugurbil, and Wu-Minn HCP Consortium. 2013. “The WU-Minn Human Connectome Project:
596 An Overview.” *Neuroimage* 80: 62–79.
- 597 Zhang, Hui, Brian B. Avants, Paul A. Yushkevich, John H. Woo, Sumei Wang, Leo F. McCluskey,
598 Lauren B. Elman, Elias R. Melhem, and James C. Gee. 2007. “High-Dimensional Spatial
599 Normalization of Diffusion Tensor Images Improves the Detection of White Matter
600 Differences: An Example Study Using Amyotrophic Lateral Sclerosis.” *IEEE Transactions on*
601 *Medical Imaging* 26 (11): 1585–97.

602